Measurement of Vertical Liquid Water Path by Means of an Airborne Radiometer and the Shortwave Albedo of Marine Low-Level Clouds during WENPEX in Japan

Y. FUJIYOSHI, Y. ISHIZAKA, AND T. TAKEDA

Institute for Hydrospheric–Atmospheric Sciences, Nagoya University, Nagoya, Japan

T. HAYASAKA AND M. TANAKA

Center for Atmospheric and Oceanic Studies, Faculty of Science, Tohoku University, Sendai, Japan

(Manuscript received 29 January 1994, in final form 21 May 1994)

ABSTRACT

Special observations were made over the southwest island area of the East China Sea from 12 to 27 January 1991 as part of the World Climate Research Program in Japan (WENPEX—Western North Pacific Cloud–Radiation Experiment). Two aircraft were used to determine the air truth of the total vertical liquid water path (LWP) using a microwave radiometer. One airplane was fitted with a 37-GHz radiometer and flew above planetary boundary layer clouds. The other flew inside the clouds with a cloud droplet spectrometer. These aircraft flew simultaneously along the same flight path when planetary boundary layer clouds were formed over the warm sea during an outbreak of cold air.

The result of the air truth of the $LWP_{radiometer}$ indicates that the 37-GHz microwave radiometer gives an estimation of the LWP accurate to 100 mg cm^{-2}. The shortwave cloud albedo was related to the $LWP_{radiometer}$. The albedo increases with the LWP, independent of cloud type, when measured just above the cloud tops. The measured albedo is nearly the same as the calculated albedo when the $LWP_{radiometer}$ is larger than 60 mg cm^{-2} but much smaller than the calculated albedo when the $LWP_{radiometer}$ is less than 40 mg cm^{-2}. Cloud-top irregularity is suggested to be the primary cause of this discrepancy. The degree of inhomogeneity of the horizontal distribution of liquid water appears to be correlated with the amount of precipitable water in the planetary boundary layer.

1. Introduction

Many researchers have studied the shortwave albedo of clouds because the reflection of solar radiation by cloudy atmospheres is the most important parameter in the study of the atmospheric energy budget. Hewson (1943) derived the equations to compute the reflected, absorbed, and transmitted fractions of sun and sky radiation incident on fog or cloud. Neiburger (1949) measured the radiative flux above, within, and below stratus clouds. Paltridge (1974) stated that a two-stream approximation could largely eliminate the discrepancy between observation and theory by taking into account the increase in liquid water content with height. On the other hand, Stephens (1978a) concluded that cloud albedo varies with the drop size distribution and is independent of the cloud's liquid water content (LWC) distribution for the fixed total liquid water path (LWP). Other theoretical investigations on the shortwave radiative properties of water clouds were done by Liou (1976) (based on the discrete ordinate method) and Slingo and Schrecker (1982) (based on the delta-Eddington multiple-scattering method).

Simple, yet accurate, parameterizations of the bulk radiative properties of various cloud types are needed for use in climate models. Stephens's (1978b) parameterization requires four variables: cloud temperature, solar zenith angle, surface albedo, and the LWP. Slingo and Schrecker (1982) presented a simple parameterization of the single-scattering properties of cloud droplets in terms of liquid water content and equivalent radius.

Detailed in situ measurements of radiative properties and microphysics are needed to ensure that the numerical models are physically realistic in various regions of the world. Slingo et al. (1982) reported the results of aircraft observations during the Joint Air–Sea Interaction Experiment performed over the Atlantic Ocean. Herman and Curry (1984) studied the radiative properties of Arctic stratus clouds. Stephens and Platt (1987) could not reconcile the reflectance spectra computed by theoretical models to those measured in a series of flights off the east coast of Australia. They suggested that the effect of cloud inhomogeneities, or the presence of an additional near-IR absorber, could explain the observed results. Foot (1988) measured the optical properties and cloud physics of a strato-

Corresponding author address: Dr. Yasushi Fujiyoshi, Institute for Hydrospheric–Atmospheric Sciences, Nagoya University, Chikusa-ku, Nagoya 464-01, Japan.

cumulus sheet that appeared over the sea near Cornwall, United Kingdom. The observed reflectances were compatible with those predicted for a plane-parallel water cloud. He concluded that the discrepancy is caused by the irregularities of cloud tops. Stephens and Tsay (1990) summarized disagreements between theoretical and observed values in both cloud absorption and reflection. King et al. (1990) observed the scattered radiation field inside stratocumulus clouds off the coast of California. His observations provide additional evidence for the existence of "anomalous absorption."

In most of the studies cited above, the LWP was obtained by integration of the averaged drop size distributions or averaged LWC. However, it is time consuming to measure the vertical profile of drop size distributions or LWC using aircraft. Since the spatial and temporal inhomogeneity of the LWP affects cloud albedo, simultaneous measurement of cloud albedo and the LWP is desirable. As described in detail later, microwave radiometers are quite useful for measuring the LWP. Derr et al. (1990) derived the LWP from the output of a ground-based microwave radiometer while measuring the broadband solar flux. In addition to the ground-based National Oceanic and Atmospheric Administration/Wave Propagation Laboratory microwave radiometer, Duda et al. (1991) measured the vertical profile of certain elements of cloud microphysics and longwave and shortwave radiation through the marine boundary layer using a National Aeronautics and Space Administration tethered balloon.

Microwave radiometry has been used more frequently in recent years to estimate the LWP. Staelin (1966) deduced the altitude distribution of water vapor and the LWP by using the inversion technique. Decker and Dutton (1970) estimated the LWP of thunderstorm cells. Aircraft observations of the LWP were made by Rosenkranz et al. (1972). Snider et al. (1980b) and Hogg et al. (1983) found good agreement in the values for the LWP measured by two independent ground-based systems using different techniques. Wei et al. (1989) investigated the accuracy of the LWP estimated by five different radiometric methods and showed that the statistical methods were more accurate than the physical methods. Researchers with the Sierra Cooperative Pilot Project have measured and studied supercooled liquid water (SLW) within winter storms. Heggli and Rauber (1988) and Reynolds and Kuciauskas (1988) measured SLW with a dual-wavelength passive microwave radiometer. The spatial and temporal evolution of SLW over the northern Colorado Rocky Mountain region has been examined by Rauber et al. (1986) and Rauber and Grant (1986). Rauber and Grant (1987) described scanning microwave radiometric and aircraft SLW measurements of a shallow, orographic cloud system in southern Utah. Sassen et al. (1990) investigated a winter mountain storm in Utah by means of multiple remote sensors and surface microphysical observations. In Japan, Liu and Takeda (1988) observed the degree of glaciation in midlevel stratiform clouds.

To estimate the role of clouds in climate, horizontal distribution of the LWP, cloud albedo, and drop size distribution should be measured simultaneously for various types of clouds in various regions of the world. Hence, special observations were made over the southwest island area of the East China Sea from 12 to 27 January 1991 as part of the World Climate Research Program in Japan (WENPEX—Western North Pacific Cloud–Radiation Experiment). In this area, planetary boundary layer clouds are formed over the warm sea during the outbreak of cold air in winter. The main topics studied were as follows:

1) Cloud climatology in the western North Pacific region
2) Distribution of clouds and their bulk radiative properties
3) Radiative properties of marine low-level clouds
4) Formation of marine low-level clouds

This paper presents the observational results concerning topic 2. Those concerning topics 1, 3, and 4 are reserved for other papers.

The following section described our observations and instruments. Section 3 presents the results of air-truth analyses of the LWP derived from an airborne microwave radiometer and characteristics of the LWP of planetary boundary layer clouds. Section 4 presents a relationship observed between the LWP and cloud albedo. The final section gives concluding remarks.

2. Observations and instruments

Two twin-engine airplanes (Cessna 404 Titan) were used in our trials. One aircraft (aircraft A) flew above clouds with a 37-GHz microwave radiometer (SPC Electronics Corporation, Japan), and two pyranometers (model MS-801, EKO Corporation, Japan). Two pyranometers were used to measure upward and downward radiative fluxes at wavelengths of 0.3–2.8 μm. The Dike-type microwave radiometer had a parabolic antenna of 20 cm in diameter and 4° in beamwidth. The brightness temperature detected ranged from 10 to 300 K with an accuracy of 0.5 K. The received power was recorded every 0.05 s and averaged for 1 s. The antenna was directed downward from the aircraft. The amounts of the LWP were derived from the radiometric data by using the algorithm presented by Takeda and Liu (1987). This method requires the following values to derive the LWP: air temperature near the sea surface, mean air temperature, and brightness temperatures emitted by a cloud and by the sea surface. As shown by Takeda et al. (1985), the microwave radiometer at 37 GHz can give a sensitive estimation of the LWP for an optically thin cloud (less

than 200 mg cm^{-2}) but becomes saturated for an optically thick cloud.

A 35-mm motor-driven camera was set and fixed pointing downward to study irregularities in the height of cloud tops using an aerial stereophotographic method. The relationship between the heights of cloud tops and the reflectance of clouds has been reported by Kikuchi et al. (1993).

The other aircraft (aircraft B) flew inside clouds with a cloud droplet spectrometer (model FSSP-100, PMS Corporation), a thermometer, and a dewpoint hygrometer. The concentration of cloud droplets with diameters ranging from 2 to 47 μm were measured by the forward-scattering spectrometer probe (FSSP). The size range was divided into 15 channels at equal widths of 3 μm. The sampling time was 1 s, and values averaged for 5 s were used as the data. Figure 1 shows the location of the southwest island and observation areas. Three types of low-level clouds appeared over the sea: stratus, stratocumulus, and cumulus. Figure 2 presents pictures of three types of clouds taken from aircraft A. Eight flights were made by aircraft A during the period from 12 to 27 January 1991. Table 1 presents a brief summary of the average shortwave downward fluxes and the maximum values of the LWP measured with the microwave radiometer on horizontal traverses. On six out of eight flights of aircraft A, simultaneous observations were made with aircraft B (2, 3, 5, 6, 7, 8).

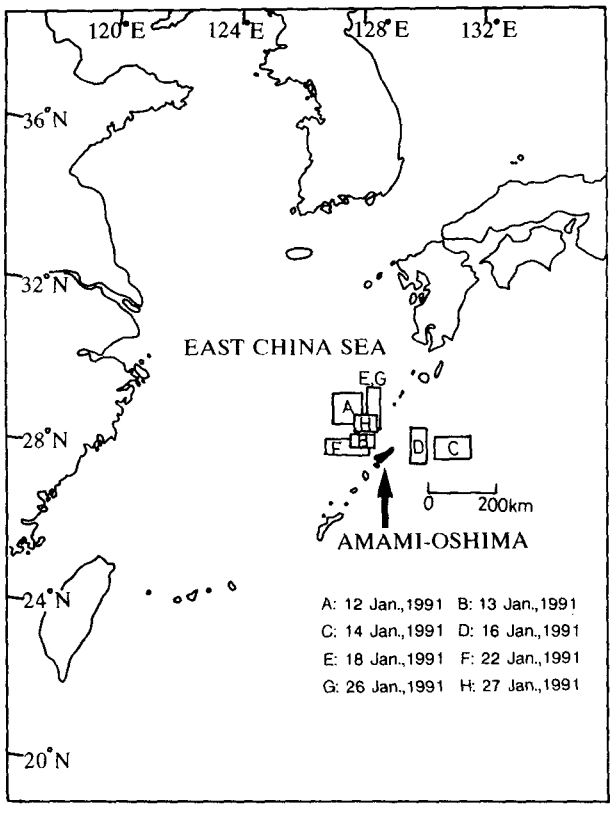

FIG. 1. The area where the observations were conducted.

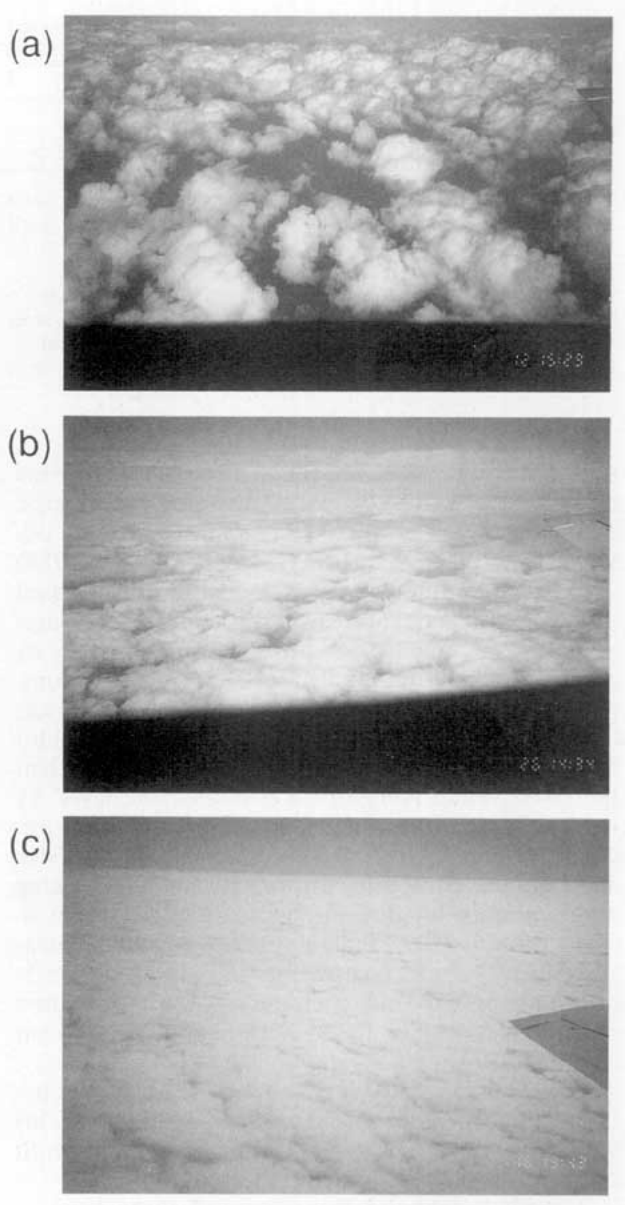

FIG. 2. Typical examples of three types of planetary boundary layer clouds that were formed over the sea during the observation period: (a) cumulus, (b) stratocumulus, and (c) stratus.

3. Air truth of the LWP derived from the microwave radiometer and the LWP of clouds

As cited above, microwave radiometers have been used to measure the LWP and SLW. However, there are only a few direct measurements of liquid water with which to compare the values derived from the radiometric data. Snider and Rottner (1982) measured SLW by means of instruments carried on an aircraft,

TABLE 1. A brief summary of the aircraft observations.

Departure–Arrival (LST)	Date	Cloud Top (m)	Cloud Depth (m)	Cloud Type	Solar zenith angle (avg) ($\mu = \cos\theta$)	Total shortwave Down (avg) (W cm^{-2})	Total shortwave Altitude (m)	$LWP_{radiometer}$ maximum (mg m^{-2})	Aircraft
1 1315–1615	12 January 1991	2700	1500	Cu, Sc, St	0.48	644	5200	55	A
2 0950–1305	13 January 1991	2000	900	Cu, Sc, St	0.58	754	3000	26	A and B
3 1015–1335	14 January 1991	2400	1200	Sc, St	0.63	796	5200	70	A and B
4 1240–1555	16 January 1991	2300	900	St	0.55	657	5200	34	A
5 1230–1535	18 January 1991	1500	500	Sc, St	0.56	719	4600	33	A and B
6 1225–1555	22 January 1991	2000	1200	Cu, Sc, St	0.57	750	5200	102	A and B
7 1235–1540	26 January 1991	2000	1000	Sc, St	0.57	666	6100	60	A and B
8 1235–1520	27 January 1991	2000	700	Cu, Sc, St	0.60	741	2600	36	A and B

that is, a Knollenberg FSSP and a Johnson–Williams hot-wire probe. They reported that the radiometric method shows somewhat higher values than were observed by the aircraft probes. Warner and Drake (1988) used two aircraft to compare the distribution of liquid water in clouds deduced from radiometric measurements below cloud base and that measured directly by penetrating the clouds at various altitudes. They compared only statistics of direct observations and retrievals from radiometer data as a percentage of cloud width for which an amount of liquid water was larger than the given value. Hill (1992) estimated the LWP by means of ground-based, dual-frequency and single-frequency microwave radiometers operating at 31.65 GHz and measured SLW using a calibrated Rosemount icing meter mounted on a research aircraft. Sheppard et al. (1991) compared the radiometric LWP with that measured by the aircraft instruments and averaged the 5.5-min averages of the radiometric LWP over the duration of aircraft ascent or descent through the stratiform cloud decks.

The results cited above revealed good agreement between the two independent measuring systems. This section describes the different way in which the air truth of the $LWP_{radiometer}$ was determined.

Aircraft B followed three types of flight patterns (stepwise, spiral, and saw-toothed) to measure vertical distributions of LWC along given flight paths. The mean length of flight paths was about 100 km. Aircraft A flew back and forth horizontally above the clouds during the flight of aircraft B and measured the LWP using the microwave radiometer along the same paths as those of aircraft B. Figure 3 shows schematics of the three flight patterns taken by aircraft B. Each of the flight patterns has advantages and disadvantages for determining the LWP_{FSSP} of a cloud.

The value of the LWP in a cloud varies greatly with time and space. The upper and lower figures in Fig. 4 show an example of a time series of the $LWP_{radiometer}$ measured on 22 January 1991. As aircraft A flew at about 70 m s^{-1}, a 5-min time interval corresponded to about 20 km on the horizontal scale. Aircraft A flew horizontally at an altitude of about 3 km and measured the $LWP_{radiometer}$ (lower figure) and then rose up to about 5 km and flew horizontally in the opposite direction along the same flight path (upper figure). The horizontal axis of the upper figure was adjusted so that the observed variation of the LWP correlates well with that of the lower figure. Aircraft B followed a spiral flight pattern numerous times in order to measure LWC of clouds. Figure 4 shows the strong variability both in space and time of the LWP in clouds, which makes it difficult to compare LWP_{FSSP} with $LWP_{radiometer}$ of an individual cloud. Additionally, $LWP_{radiometer}$ of a cloud may not be representative, because the microwave radiometer measured only the LWP along a narrow flight path, as described by Warner and Drake (1988). This is also the case for the

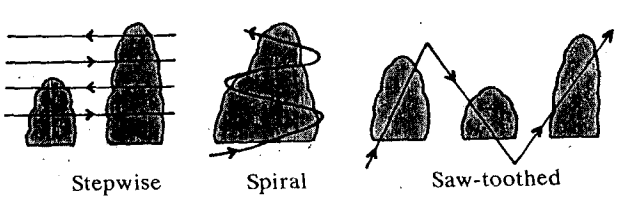

FIG. 3. Schematic of the three flight patterns.

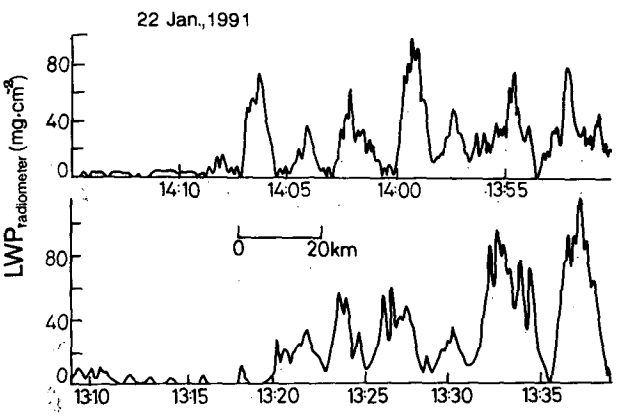

FIG. 4. An example of a time series of the $LWP_{radiometer}$.

LWC with FSSP. To avoid these difficulties we compared the maximum value of $LWP_{radiometer}$ ($LWP_{max;rad}$) with $LWP_{max;FSSP}$. Figure 5 shows all the values of LWC_{FSSP} measured from 1357 to 1438 JST 22 January 1991. Figure 6 presents the vertical profiles of air temperature and relative humidity within and outside the clouds. An envelope curve was made to include all data. Strong temperature inversion was noted just below the level of 2 km, and relative humidity decreased sharply above the inversion level. Aircraft B followed the spiral and saw-toothed patterns. The values of LWC_{FSSP} varied greatly, even at the same flight level. The $LWP_{max;FSSP}$ corresponds to the area inside the envelope curve. The LWP of fully developed and mature cloud should be the same as $LWP_{max;FSSP}$.

The $LWP_{max;rad}$ and the $LWP_{max;FSSP}$ are compared in Fig. 7. Though the number of points is quite limited, the microwave radiometer and the cloud droplet spectrometer produce almost the same values for the LWP.

If a saturated air parcel rises adiabatically from cloud base to cloud top, LWP_a is calculated by using a vertical air temperature profile. The calculated value of LWP_a should be the maximum value that the cloud layer can support. Thus far, it is unclear whether or not LWC is the same as the adiabatic value (LWC_a). Warner (1955) measured LWC of isolated cumulus or stratocumulus clouds and found that 1) the peak value of LWC was fairly reproducible from traverse to traverse at a fixed height, even though the amount of LWC at a given height varied greatly during the traverse through a cloud, and 2) the value of LWC/LWC_a generally decreased with height above cloud base and was always less than 1. In contrast, Heymsfield et al. (1978) reported that the ratio of LWC/LWC_a was highly variable and did not generally indicate a systematic decrease with altitude increase. Moist-adiabatic cores were found in cumulus congestus clouds where LWC/LWC_a was about 1. The measurements of LWC of marine stratocumulus made by Slingo et al. (1982) and Duda et al. (1991) revealed an LWC/LWC_a value close to 1.

If aircraft A flew above at least one fully developed cloud or one moist-adiabatic core, $LWP_{max;rad}$ should be the same as LWP_a. Wielicki and Welch (1986) reported that the cumulus clouds were often multicelled, even in clouds as small as 1 km in diameter. Figure 4 indicates that a number of small peaks (1–3 km) were embedded in each large peak (about 10 km). These small peaks correspond to convective cores in a cloud. Therefore, the above assumption may be valid when numerous clouds of the same type are present along the flight path. Figure 8 shows the comparison between $LWP_{max;rad}$ along each flight path and LWP_a. The maximum value of the $LWP_{radiometer}$ measured along the all flight paths was chosen as $LWP_{max;rad}$ in Fig. 8, and that measured above the area where aircraft B measured LWP_{FSSP} was chosen as $LWP_{max;rad}$ in Fig. 7. Thus, the values of $LWP_{max;rad}$ in Fig. 8 are equal to or larger than those in Fig. 7. The ratio between $LWP_{max;rad}$ and LWP_a is nearly 1 when LWP_1 is smaller than 100 mg cm^{-2} and is smaller than 1 when LWP_a is larger than 100 mg cm^{-2}. This result suggests that the microwave radiometer gives a good estimation of the LWP to at least less than 100 mg cm^{-2}.

Clouds exert a large influence not only on the atmospheric radiation budget but also on the fluxes of sensible and latent heats. Even small changes in the amount of global-scale cloud coverage could lead to significant climate perturbations. Cloud feedback depends on the change in both the fractional cloud cover

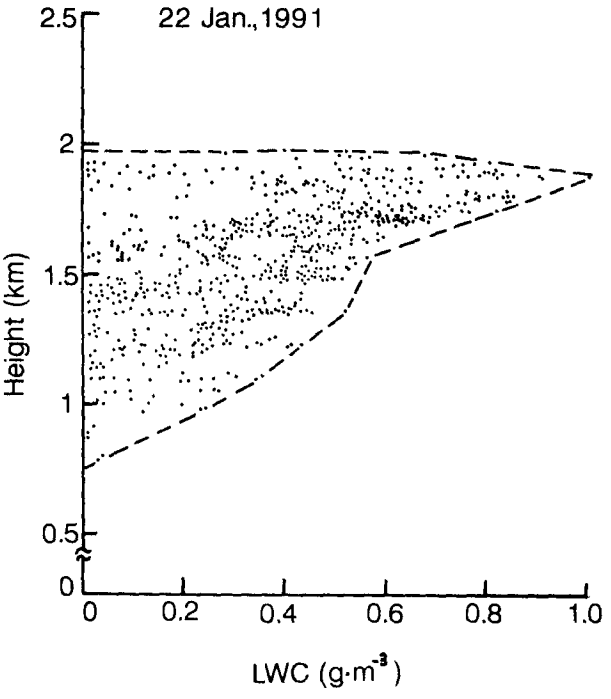

FIG. 5. A vertical distribution of LWC measured from 1357 to 1438 JST 22 January 1991. Each point represents LWC measured with FSSP averaged for 5 s. The dashed line indicates the envelope of all points.

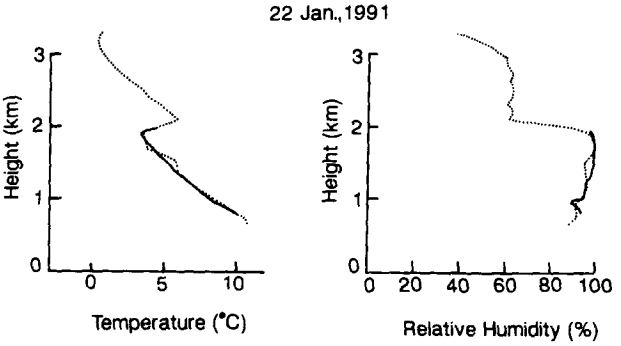

FIG. 6. Mean vertical profiles of air temperature and relative humidity on 22 January 1991. Those measured within and outside of clouds are shown by dotted and thick lines, respectively.

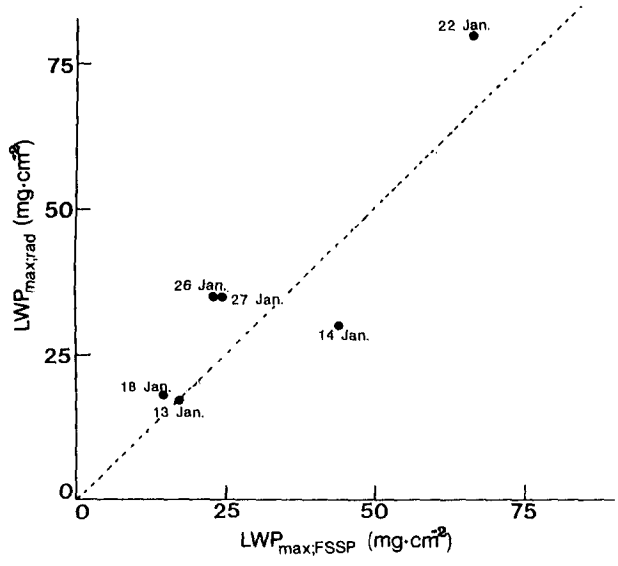

FIG. 7. Comparison of $LWP_{max;rad}$ and $LWP_{max;FSSP}$.

and the cloud radiative properties. The exponential size distributions of cumulus clouds have been reported by Plank (1969) and Hozumi et al. (1982) using aerial photographs. Using Landsat data, Wielicki and Welch (1986) derived nearly the same cloud-size distributions. Taylor and Ghan (1992) modified the National Center for Atmospheric Research (NCAR) Community Climate Model, so that the cloud radiative properties are functions of LWC, to study the LWC feedback effect on climate sensitivity. They suggested that the actual change in albedo would depend on the details of the frequency distribution of clouds of differing LWP. Although radiative properties and latent heat release of clouds are primarily dependent on the LWP, the LWP of clouds and the horizontal distribution of the LWP have not been studied well.

As shown in Fig. 8, the value of $LWP_{max;rad}$ was close to that of LWP_a: most of the values of the $LWP_{radiometer}$ were smaller than LWP_a. The histograms of the frequency of the appearance of the LWP along the flight paths were investigated with a parameter of $LWP_{max;rad}$. LWP_a is considered a proper parameter characterizing a planetary boundary layer. In Figs. 7 and 8 the comparisons were made only when aircraft A and B flew simultaneously along the same flight paths. However, aircraft B did not always measure temperature and humidity profiles along the flight paths of aircraft A. There were cases when aircraft A flew but aircraft B did not and vice versa, or when aircraft A flew different paths from those of aircraft B. Therefore, the data are quite limited when LWP_a is used as a parameter. As shown in Fig. 8, $LWP_{max;rad}$ is proportional to LWP_a. Qualitative characteristics would not be changed even where $LWP_{max;rad}$ was used instead of LWP_a as a parameter.

Figure 9 shows the histograms of the frequency of the appearance of peak values of the $LWP_{radiometer}$ along each flight path in order of the magnitude of $LWP_{max;rad}$. Here, the peak values of the $LWP_{radiometer}$ are divided by $LWP_{max;rad}$. This procedure allows comparison of the shapes of histograms with each other regardless of $LWP_{max;rad}$. The number of peaks counted is written in parentheses and the value of $LWP_{max;rad}$ is presented in each figure. The histograms can be approximated by the gamma distribution function. Figure 8 also shows the curves fitted to the histograms (dotted line). The appearance frequency of clouds whose LWP was close to LWP_a was studied by counting the number of clouds with LWP values greater than 0.9 $LWP_{max;rad}$ ($LWP_{>90\%}$). Figure 10 shows the dependency of $LWP_{>90\%}$ on $LWP_{max;rad}$. The figure shows clearly that $LWP_{>90\%}$ is inversely proportional to $LWP_{max;rad}$. Thus, the chance of measuring the LWP of fully developed clouds or moist-adiabatic cores decreases with increasing LWP_a, since $LWP_{max;rad}$ was nearly equal to LWP_a as shown in Fig. 8.

Figures 9 and 10 suggest that the value of the LWP at which the appearance frequency is maximum is expected to approach LWP_a as LWP_a decreases. In fact, the normalized LWP at which the appearance frequency is maximum ($LWP_{max;freq}$) decreases exponentially with an increase in $LWP_{max;rad}$, as shown in Fig. 11. The results shown in Figs. 9, 10, and 11 indicate that the number of clouds with an LWP close to LWP_a decreases as LWP_a increases. In other words, the degree of inhomogeneity of the horizontal distribution of liquid water increases with increasing amounts of precipitable water in the planetary boundary layer.

4. Shortwave broadband albedo and the LWP of clouds

Figure 12 shows a time series of upward and downward fluxes and the $LWP_{radiometer}$ on 22 January 1991.

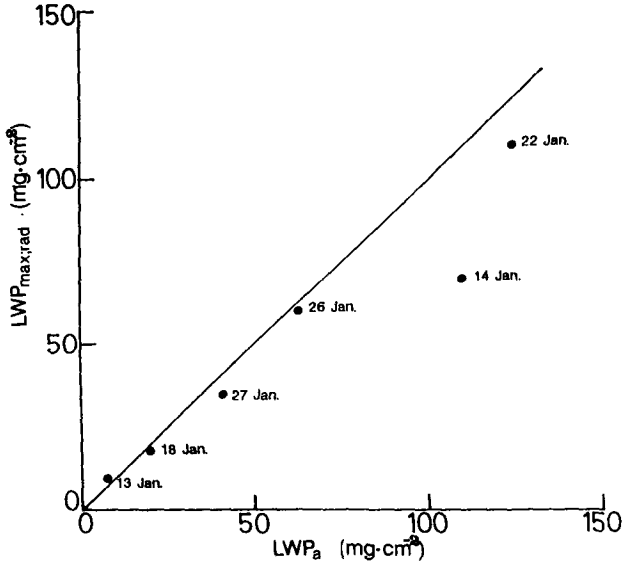

FIG. 8. Comparison of $LWP_{max;rad}$ and LWP_a.

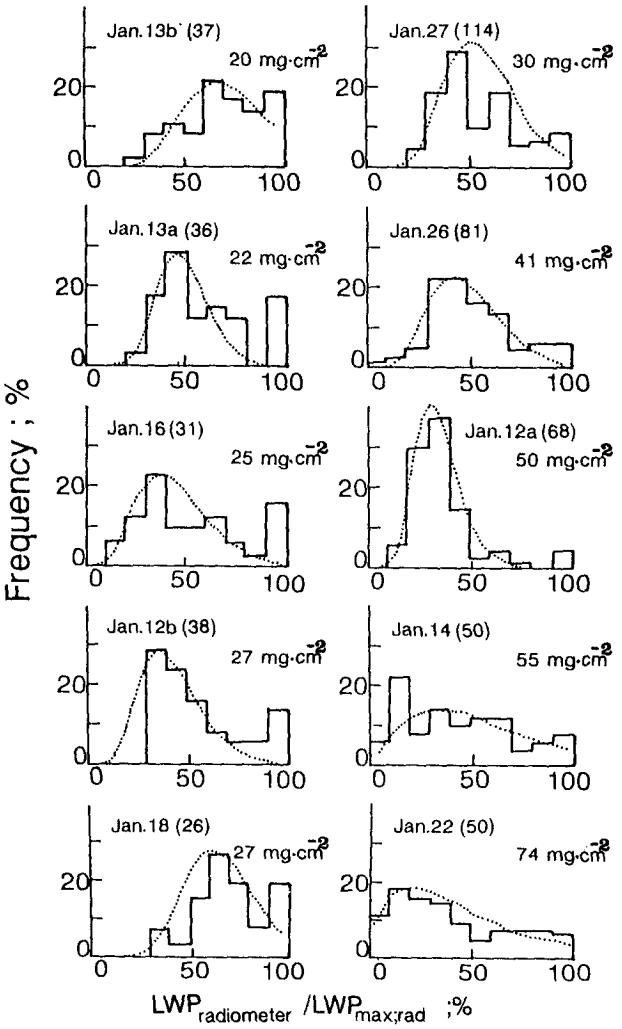

FIG. 9. Histograms of the frequency of appearance of peak values of normalized $LWP_{radiometer}$. The numeral in each figure represents $LWP_{max;rad}$. The number of peaks counted is written in parentheses.

Since aircraft A flew horizontally just above the clouds (about 100 m above the cloud tops), the absorption of shortwave radiation by gases can be neglected between the flight level and the level of the cloud tops. Therefore, the cloud albedo is calculated by dividing upward flux by downward flux. As seen in Fig. 12, there are seven peaks in the time series. Comparison was made between the peak values of the cloud albedo and those of the $LWP_{radiometer}$ for the following reasons. When cloud albedo is compared to the LWP, it is necessary to take into account the difference between the viewing angle of the pyranometer (hemisphere) and that of the microwave radiometer (4°). The cloud albedo will change whether or not the sampling area of the pyranometer is fully covered by clouds, even though the microwave radiometer gives the same LWP, and vice versa. Therefore, the values of albedo and the LWP that were measured near the periphery of clouds were discarded to minimize the risk of such an error.

Figures 13 and 14 show the relationships between cloud albedo and the $LWP_{radiometer}$. The observed clouds were classified into three types: stratus (St), cumulus (Cu), and stratocumulus (Sc). The cloud amount of St was 100%. The Sc cloud type was subjectively classified into two types, Sc_1 and Sc_2, when the space between clouds was apparent and when most of the area was covered by clouds, respectively (Fig. 2 presents a typical example of the Sc_2 type). The types of clouds in Figs. 13 and 14 are Cu + Sc_1 and St + Sc_2, respectively. Cloud albedo increases with an increase in the LWP and approaches 0.83. The difference between the cloud albedo of the two regression lines (thin lines) is less than 0.05 and is especially small when the $LWP_{radiometer}$ is less than 20 mg cm^{-2}. This result indicates that the difference in cloud amount has at least a small effect on the relationship presented in Figs. 13 and 14.

The change in cloud albedo with the LWP was calculated using Stephens's (1978a,b) parameterization scheme. The solar zenith angle ranged from 0.55 to 0.62 (see Table 1) and the effective radius was assumed to be 4.7 μm, which is the representative value during the observations. The transfer of solar radiation in a plane-parallel scattering atmosphere and the absorption of solar radiation by water vapor were calculated according to the methods of Nakajima and Tanaka (1986) and Asano and Uchiyama (1987), respectively. The calculated cloud albedo lies between two dotted lines (18 and 22 January 1991). The value is close to the measured albedo when the $LWP_{radiometer}$ is larger than 60 mg cm^{-2}. The difference between calculated and measured cloud albedo is large when the $LWP_{radiometer}$ is less than 40 mg cm^{-2}. In our observations, the effective radius occurred in the size range of 3.5–6.0 μm. Slingo (1989) showed that, when the LWP is the same, a 2-μm increase in the equivalent radius causes a greater than 10% decrease in the re-

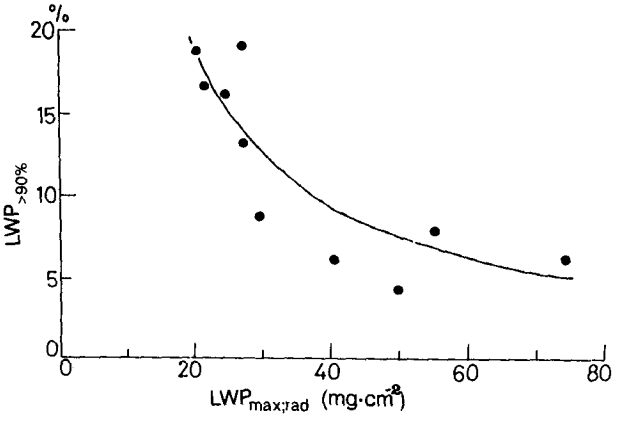

FIG. 10. Relationship between $LWP_{>90\%}$ and $LWP_{max;rad}$.

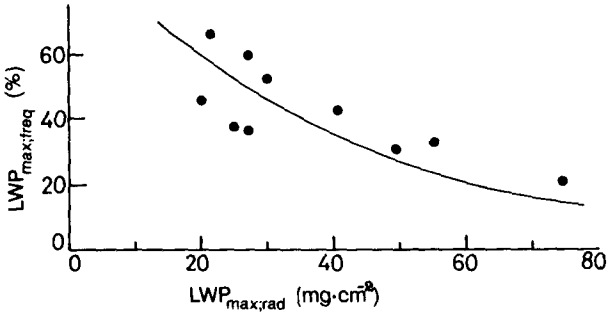

FIG. 11. Relationship between $LWP_{max;freq}$ and $LWP_{max;rad}$.

flectivity of clouds. Thus, the effect of the effective radius might explain the difference between calculated and measured cloud albedo. However, the values of measured cloud albedo show the same tendency for all cases, and thus, the difference is not caused mainly by this effect.

The calculation is based on the assumption that clouds are plane parallel. The shape of clouds is generally not flat, and cloud geometry should affect the intensity of upward solar flux. Neiburger (1949) suggested that the anisotropy of the radiation could explain the discrepancy between theory and his observations. Weinman and Swarztrauber (1968) and Wendling (1977) showed that a deeply striated medium of a given mean optical thickness has a lower mean albedo than

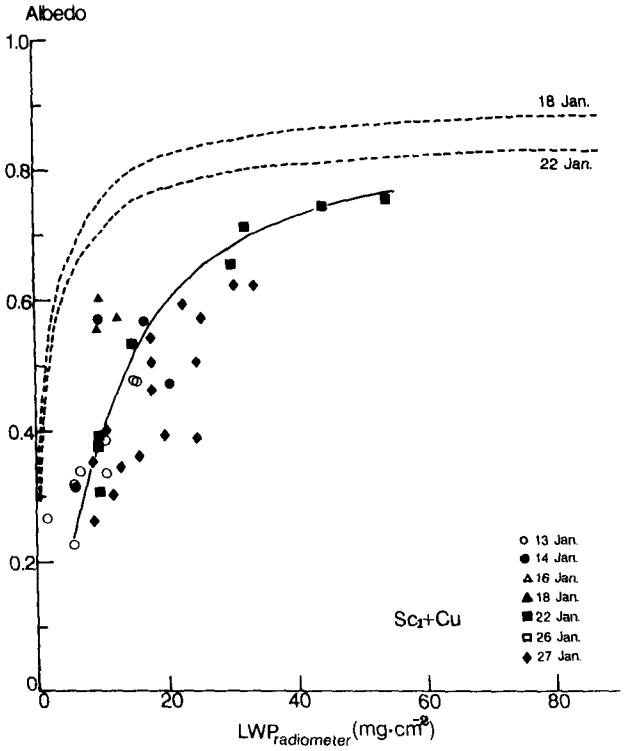

FIG. 13. Dependency of the albedo of type Cu + Sc_t clouds on the $LWP_{radiometer}$ measured just above the cloud tops. The thin line represents a regression line. Two dotted lines represent the cloud albedo, calculated using Stephens's parameterization scheme, on 18 and 22 January 1991.

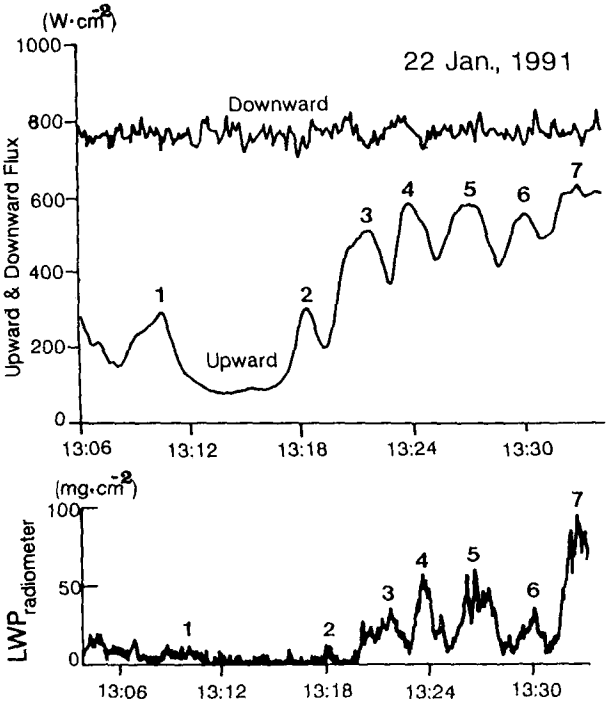

FIG. 12. Time series of the $LWP_{radiometer}$ (bottom figure), and upward and downward total solar fluxes (upper figure) on 22 January 1991.

a horizontally homogeneous medium of the same mean optical thickness. The scattering of shortwave radiation by finite clouds was theoretically studied by McKee and Cox (1974). Their calculations illustrate that cubic clouds reflect a much smaller fraction of radiation incident on them than do infinite horizontal clouds. These studies could explain the difference between calculated and measured cloud albedo shown in Figs. 13 and 14. During our observations, Kikuchi et al. (1993) set a 35-mm motor-driven camera at the bottom of aircraft A to study the irregularities in the heights of the cloud tops. They reported that the cloud albedo was low when the cloud tops were sharp and jagged in shape.

The influence of irregular cloud tops on upward solar flux decreases with an increase in the distance between the aircraft and the clouds. Figure 15 shows a relationship between the cloud albedo and the $LWP_{radiometer}$ measured at a high altitude (about 3 km above the cloud tops). The types of clouds are Sc_2 and St, in order to neglect the effect of the cloud amount on the averaged cloud albedo of the area. The values of cloud albedo measured at lower flight levels are larger than those at higher flight levels. This is because the downward solar flux decreases with a decrease in altitude and upward solar flux decreases with an increase in

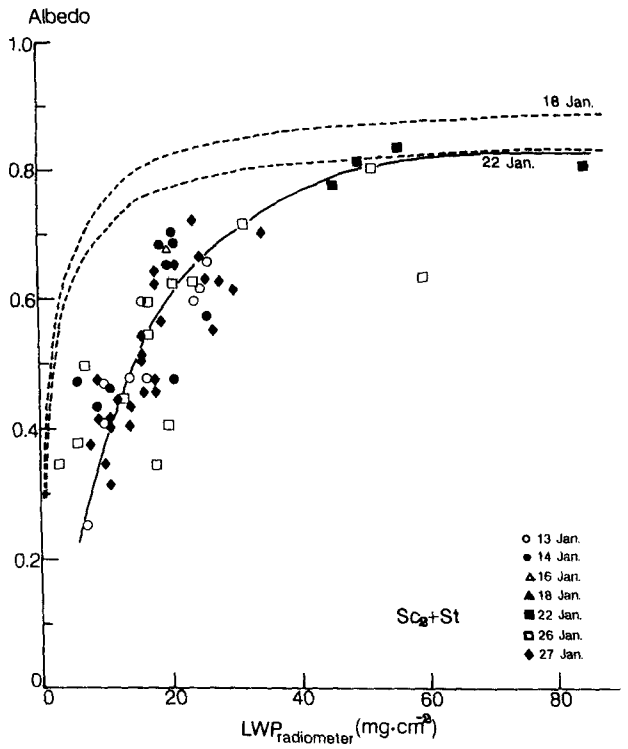

FIG. 14. Same as Fig. 13 except for St + Sc_2 cloud types.

altitude due to gaseous absorption. Nevertheless, the values of cloud albedo in Fig. 15 are larger than those in Figs. 13 and 14 when the $LWP_{radiometer}$ is less than 20 mg cm^{-2}. Consequently, the results shown in Fig. 15 and presented by Kikuchi et al. (1993) indicate that the irregularity in cloud tops decreases the albedo of an optically thin cloud when a measurement is made just above the top of the cloud.

5. Concluding remarks

The result of the air-truth analysis of the $LWP_{radiometer}$ indicates that the 37-GHz microwave radiometer gives a good estimation of the LWP to at least less than 100 mg cm^{-2}. The difference between the LWP_{FSSP} and $LWP_{radiometer}$ is caused primarily by two factors. First, the odds of measuring the LWP of fully developed clouds would decrease with an increase in the LWP. Second, in an inversion-capped cloud layer, the convective activity generally becomes strong with increasing LWP_a. Entrainment of surrounding dry air into clouds would be extensive when convective activity in clouds is strong. Thus, the LWP of a convective cloud is smaller than LWP_a when LWP_a is large.

Shortwave cloud albedo is related to the $LWP_{radiometer}$. The albedo increases with the LWP, independent of cloud type, when measured just above the cloud tops. The measured albedo is nearly the same as the calculated albedo when the $LWP_{radiometer}$ is larger than 60 mg cm^{-2}, but is much smaller than the calculated albedo when the $LWP_{radiometer}$ is less than 40 mg cm^{-2}. Cloud-top irregularity is suggested to be the primary cause of this discrepancy. Kikuchi et al. (1993) have described the structure and reflectance of winter maritime clouds in detail. Hayasaka et al. (1994, 1995) will compare measured cloud albedos in the visible and near-IR spectral region with calculated values and will discuss the discrepancy in detail.

It is interesting that the histograms of the frequency of the appearance of peak values of the $LWP_{radiometer}$ are approximated by the gamma distribution function and not by the exponential function. The result that the number of peaks of the $LWP_{radiometer}$ decreases as the $LWP_{radiometer}$ decreases suggests that even small clouds have some finite value of the LWP. When clouds dissipate, they generally do not shrink their size but become diffuse as a whole. Therefore, the result also suggests that small clouds do not correspond to the dissipating stage of larger clouds. Another interesting feature of the horizontal distribution of the LWP is that $LWP_{>90\%}$ decreases with $LWP_{max;rad}$ or LWP_a. One explanation of the result is as follows: When there is a large amount of precipitable water in the planetary boundary layer, strong convective clouds tend to develop. Under these conditions, the stability of the surrounding air would change due to the compensating downward air motion. Therefore, clouds of various horizontal and vertical scales would form nearby. The coexistence of various sizes of clouds indicates inho-

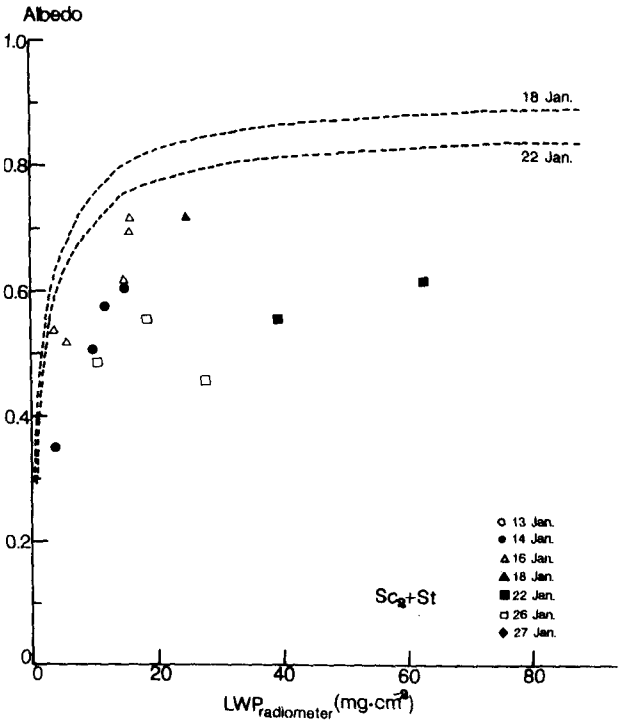

FIG. 15. Same as Fig. 14 except measured at higher flight levels.

mogeneous horizontal distribution of water vapor and liquid water. If such inhomogeneity does not occur, the value of $LWP_{max;freq}$ would increase with LWP_a. However, $LWP_{max;freq}$ decreases with LWP_a. The inhomogeneity in the LWP would correspond to an increase in the standard deviation of the size distribution of clouds. Although Plank (1969), Hozumi et al. (1982), and Wielicki and Welch (1986) studied the size distribution of clouds, they did not examine the standard deviation of the size distribution and the relationship between the standard deviation and static stability or LWP_a of the air where the clouds were formed. Cloud size and the LWP distributions should be related to the static stability or LWP_a.

Since, in the present study, the values of the LWP were measured only along the flight path, the distribution presented here may differ from the aerial distribution of LWP. Additional studies of the aerial horizontal distribution of the LWP are required for a more complete understanding of these phenomena.

Acknowledgments. This work was supported by the Ministry of Education, Science and Culture of Japan. The authors wish to thank Dr. G. Liu for assistance with the calculation of the $LWP_{radiometer}$. We acknowledge Drs. Y. Asuma and T. Endoh from Hokkaido University, and Dr. K. Kato from Nagoya University for their assistance in aircraft observations. We are grateful to Mr. Kurahashi who assisted us in calculating LWP_{FSSP}.

REFERENCES

Asano, S., and A. Uchiyama, 1987: Application of an extended ESFT method to calculation of solar heating rates by water vapor absorption. *J. Quant. Spectrosc. Radiat. Transfer,* **38,** 147–158.

Decker, M. T., and E. J. Dutton, 1970: Radiometric observations of liquid water in thunderstorm cells. *J. Atmos. Sci.,* **27,** 785–790.

Derr, V. E., R. S. Stone, L. S. Fedor, and H. P. Hanson, 1990: A parameterization for the shortwave transmissivity of stratiform water clouds based on empirical data and radiative transfer theory. *J. Atmos. Sci.,* **47,** 2774–2783.

Duda, D. P., G. L. Stephens, and S. K. Cox, 1991: Microphysical and radiative properties of marine stratocumulus from tethered balloon measurements. *J. Appl. Meteor.,* **30,** 170–186.

Foot, J. S., 1988: Some observations of the optical properties of clouds. I: Stratocumulus. *Quart. J. Roy. Meteor. Soc.,* **114,** 129–144.

Hayasaka, T., M. Kuji, and M. Tanaka, 1994: Air-truth validation of cloud albedo estimated from NOAA AVHRR data. *J. Geophys. Res.,* **99,** 18 685–18 693.

——, T. Nakajima, Y. Fujiyoshi, Y. Ishizaka, T. Takeda, and M. Tanaka, 1995: Geometrical thickness, liquid water content, and radiative properties of stratocumulus clouds observed in the western North Pacific. *J. Appl. Meteor.,* **34,** 460–470.

Heggli, M. F., and R. M. Rauber, 1988: The characteristics and evolution of super-cooled water in wintertime storms over the Sierra Nevada: A summary of microwave radiometric measurements taken during the Sierra Cooperative Pilot Project. *J. Appl. Meteor.,* **27,** 989–1015.

Herman, G. F., and J. A. Curry, 1984: Observational and theoretical studies of solar radiation in Arctic stratus clouds. *J. Climate Appl. Meteor.,* **23,** 5–24.

Hewson, E. W., 1943: The reflection, absorption, and transmission of solar radiation by fog and cloud. *Quart. J. Roy. Meteor. Soc.,* **69,** 47–62.

Heymsfield, A. J., P. N. Johnson, and J. E. Dye, 1978: Observations of moist adiabatic ascent in northeast Colorado cumulus congestus clouds. *J. Atmos. Sci.,* **35,** 1689–1703.

Hill, G. E., 1992: Further comparisons of simultaneous airborne and radiometric measurements of supercooled liquid water. *J. Appl. Meteor.,* **31,** 397–401.

Hogg, D. C., F. O. Guiraud, J. B. Snider, M. T. Decker, and E. R. Westwater, 1983: A steerable dual-channel microwave radiometer for measurement of water vapor and liquid in the troposphere. *J. Appl. Meteor.,* **22,** 789–806.

Hozumi, K., T. Harimaya, and C. Magono, 1982: The size distribution of cumulus clouds as a function of cloud amount. *J. Meteor. Soc. Japan,* **60,** 691–699.

Kikuchi, K., and Coauthors, 1993: Structure and reflectance of winter maritime stratocumulus clouds. *J. Meteor. Soc. Japan,* **71,** 715–731.

King, M. D., L. F. Radke, and P. V. Hobbs, 1990: Determination of the spectral absorption of solar radiation by marine stratocumulus clouds from airborne measurements within clouds. *J. Atmos. Sci.,* **47,** 894–907.

Liou, K. N., 1976: On the absorption, reflection and transmission of solar radiation in cloudy atmosphere. *J. Atmos. Sci.,* **33,** 798–805.

Liu, G., and T. Takeda, 1988: Observation of the degree of glaciation in middle-level stratiform clouds. *J. Meteor. Soc. Japan,* **66,** 645–660.

McKee, T. B., and S. K. Cox, 1974: Scattering of visible radiation by finite clouds. *J. Atmos. Sci.,* **31,** 1885–1892.

Nakajima, T., and M. Tanaka, 1986: Matrix formulations for the transfer of solar radiation in a plane-parallel scattering atmosphere. *J. Quant. Spectrosc. Radiat. Transfer,* **35,** 13–21.

Neiburger, M., 1949: Reflectivity, absorption, and transmission of insolation by stratus cloud. *J. Meteor.,* **6,** 98–104.

Paltridge, G. W., 1974: Infrared emissivity, short-wave albedo, and the microphysics of stratiform water clouds. *J. Geophys. Res.,* **20,** 4053–4058.

Plank, V. G., 1969: The size distribution of cumulus clouds in representative Florida populations. *J. Appl. Meteor.,* **8,** 46–67.

Rauber, R. M., and L. O. Grant, 1986: The characteristics and distribution of cloud water over the mountains of northern Colorado during wintertime storms. Part II: Spatial distribution and microphysical characteristics. *J. Climate Appl. Meteor.,* **25,** 489–504.

——, and ——, 1987: Supercooled liquid water structure of shallow orographic cloud system in southern Utah. *J. Climate Appl. Meteor.,* **26,** 208–215.

——, ——, D. Feng, and J. B. Snider, 1986: The characteristics and distribution of cloud water over the mountains of northern Colorado during wintertime storms. Part I: Temporal variations. *J. Climate Appl. Meteor.,* **25,** 468–488.

Reynolds, D. W., and A. P. Kuciauskas, 1988: Remote and in situ observations of Sierra Nevada winter mountain clouds: Relationships between mesoscale structure, precipitation and liquid water. *J. Appl. Meteor.,* **27,** 140–156.

Rosenkranz, P. W., and Coauthors, 1972: Microwave radiometric measurements of atmospheric temperature and water from an aircraft. *J. Geophys. Res.,* **77,** 5833–5844.

Sassen, K., A. W. Huggins, A. B. Long, J. B. Snider, and R. J. Meitin, 1990: Investigation of a winter mountain storm in Utah. Part II: Mesoscale structure, supercooled liquid water development, and precipitation processes. *J. Atmos. Sci.,* **47,** 1323–1350.

Sheppard, B. E., R. E. Stewart, and G. A. Isaac, 1991: Nonlinear optimal estimation of temperature and integrated water vapor and liquid using a ground-based microwave radiometer in coastal winter storms. *J. Atmos. Oceanic Technol.,* **8,** 812–825.

Slingo, A., 1989: A GCM parameterization for the shortwave radiative properties of water clouds. *J. Atmos. Sci.,* **46,** 1419–1427.

——, and H. M. Schrecker, 1982: On the shortwave radiative properties of stratiform water clouds. *Quart. J. Roy. Meteor. Soc.,* **108,** 407–426.

——, S. Nicholls, and J. Schmetz, 1982: Aircraft observations of marine stratocumulus during JASIN. *Quart. J. Roy. Meteor. Soc.,* **108,** 833–856.

Snider, J. B., and D. Rottner, 1982: The use of microwave radiometry to determine a cloud seeding opportunity. *J. Appl. Meteor.,* **21,** 1286–1291.

——, H. M. Burdick, and D. C. Hogg, 1980a: Cloud liquid measurement with a ground-based microwave instrument. *Radio Sci.,* **15,** 683–693.

——, F. O. Guiraud, and D. C. Hogg, 1980b: Comparison of cloud liquid content measured by two independent ground-based systems. *J. Appl. Meteor.,* **19,** 577–579.

Staelin, D. H., 1966: Measurements and interpretation of the microwave spectrum of the terrestrial atmosphere near 1-centimeter wavelength. *J. Geophys. Res.,* **71,** 2875–2881.

Stephens, G. L., 1978a: Radiation profiles in extended water clouds. I: Theory. *J. Atmos. Sci.,* **35,** 2111–2122.

——, 1978b: Radiation profiles in extended water clouds. II: Parameterization schemes. *J. Atmos. Sci.,* **35,** 2123–2132.

——, and C. M. R. Platt, 1987: Aircraft observations of the radiative and microphysical properties of stratocumulus and cumulus cloud fields. *J. Climate Appl. Meteor.,* **26,** 1243–1269.

——, and S. C. Tsay, 1990: On the cloud absorption anomaly. *Quart. J. Roy. Meteor. Soc.,* **116,** 671–704.

Takeda, T., and G. Liu, 1987: Estimation of atmospheric liquid-water amount by Nimbus 7 SMMR data—A new method and its application to the Western North-Pacific region. *J. Meteor. Soc. Japan,* **65,** 931–947.

——, ——, and M. Wada, 1985: Estimation of liquid water amount by microwave radiometer. *Mem. Natl. Inst. Polar Res. Spec. Issue,* **39,** 97–107.

Taylor, K. E., and S. J. Ghan, 1992: An analysis of cloud liquid water feedback and global climate sensitivity in a general circulation model. *J. Climate,* **5,** 907–919.

Warner, J., 1955: The water content of cumuliform cloud. *Tellus,* **4,** 449–457.

——, and J. F. Drake, 1988: Field tests of an airborne remote sensing technique for measuring the distribution of liquid water in convective cloud. *Tellus,* **5,** 833–843.

Wei, C., H. G. Leighton, and R. R. Rogers, 1989: A comparison of several radiometric methods of deducing path-integrated cloud liquid water. *J. Atmos. Oceanic Technol.,* **6,** 1001–1012.

Weinman, J. A., and P. N. Swarztrauber, 1968: Albedo of a striated medium of isotropically scattering particles. *J. Atmos. Sci.,* **25,** 497–501.

Wendling, P., 1977: Albedo and reflected radiance of horizontally inhomogeneous clouds. *J. Atmos. Sci.,* **34,** 642–650.

Wielicki, B. A., and R. M. Welch, 1986: Cumulus cloud properties derived using Landsat satellite data. *J. Climate Appl. Meteor.,* **25,** 261–276.